RSC Sustainability

ROYAL SOCIETY OF CHEMISTRY

PAPER

View Article Online
View Journal | View Issue

Cite this: *RSC Sustainability*, 2025, **3**, 5167

Green synthesis of spiro-barbiturates: advancing sustainable chemistry and drug design research

Devanshi Magoo, *[a] Smriti Sharma,[b] Anju Srivastava,[a] Shruti Gupta,[c] Reena Jain,[a] Sriparna Dutta,[a] Kalawati Meena,[d] Soma M. Ghorai,[e] Simran Nischal,[a] Kirti[a] and R. K. Sharma [a]

Received 15th May 2025
Accepted 26th September 2025

DOI: 10.1039/d5su00343a

rsc.li/rscsus

Through this research, we have established an environmentally friendly and sustainable approach for the synthesis of spirobarbiturate (SB) derivatives, which hold significant potential in the field of medicinal chemistry. The methodology emphasizes the design of safer synthetic routes, judicious selection of reagents, waste minimization, and the advantages of using green solvents. The spirobarbiturate derivatives were synthesized utilizing a one-pot, three-component reaction of arylidene-1,3-dimethylpyrimidine-2,4,6(1*H*,3*H*,5*H*)-triones with dimethylacetylenedicarboxylate and triphenylphosphine in cyclopentyl methyl ether (CPME), a bio-based green solvent, under room temperature conditions. The synthesized compounds were characterized and *in silico* assessed by molecular docking and molecular dynamics (MD) simulations using GABA(A) and NMDA receptors. The methoxy-substituted spirobarbiturate showed the strongest binding and highest dynamic stability with the GABA(A) receptor, as determined by MMGBSA free energy calculations. The presented methodology highlights the importance of employing eco-friendly synthetic techniques in drug design research while the results of docking and simulation studies are indicative of exploring the potential use of synthesized compounds as neuronal drugs. Furthermore, this paper also provides the methodology of calculations for the 'green quotient' of the protocol employed, thereby advocating the promotion of green chemistry practices and skills in the newer generation of chemists.

Sustainability spotlight

This work features an environmentally friendly and sustainable approach for the synthesis of pharmacologically significant spirobarbiturate motifs and their molecular simulations for assessment as potential neuronal drugs. The protocol employs CPME as a bio-based green solvent that has a prominent position in the GSK and CHEM21 solvent selection guides. Additionally, the protocol's 'green quotient' has been quantitatively evaluated through relevant green chemistry metrics such as atom economy, carbon efficiency, reaction mass efficiency, *E*-factor, *etc.*, reinforcing the importance of integrating sustainable development principles and skills into the training of future chemists. Designing benign syntheses of spirobarbiturate compounds and their *in silico* evaluation bridges green chemistry with drug design research, fostering interdisciplinary collaboration and laying the groundwork for future breakthroughs that could benefit both the environment and society at large.

Introduction

Green chemistry holds a vital place in the chemical community research as it aims at reducing or eliminating the use or generation of hazardous substances in the design, manufacture, and applications of chemical products.[1] With the elevating levels of pollution, it has become increasingly relevant to incorporate green chemistry into modern laboratory practices.[2] Guided by the twelve principles, it enables researchers to challenge their traditional chemical thinking and design more environmentally benign routes for previously reported reactions.[3]

This work features the synthesis of spiro-barbiturates under environmentally benign reaction conditions. The synthesized compounds were subjected to *in silico* analysis, including molecular docking and molecular dynamics (MD) simulations, focusing on GABA(A) receptors, *N*-methyl-D-aspartate receptors (NMDARs), and glutamate receptors.[4]

Balancing neurotransmitters like glutamate and GABA is critical for maintaining homeostasis and overall well-being.[5] Barbiturates, once widely used for their anesthetic properties by

[a]*Department of Chemistry, Hindu College, University of Delhi, Delhi-110007, India. E-mail: devanshimagoo@hinducollege.ac.in*

[b]*Department of Chemistry, Miranda House College, University of Delhi, Delhi-110007, India*

[c]*Department of Chemistry, University of Delhi, Delhi-110007, India*

[d]*Department of Chemistry, Dyal Singh College, University of Delhi, Delhi-110003, India*

[e]*Department of Zoology, Hindu College, University of Delhi, Delhi-110007, India*

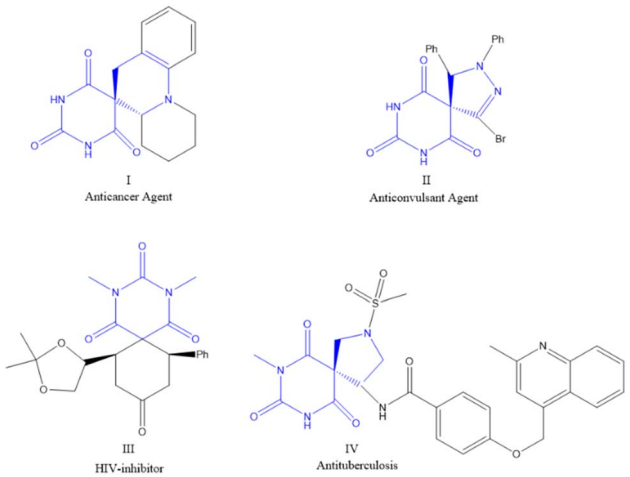

Fig. 1 Pharmacologically significant spirocyclic ring systems.

modulating GABA(A) receptors,[6] have fallen out of favor due to their high abuse potential.[7] This has spurred interest in developing safer analogues, such as spirobarbiturates, which retain therapeutic benefits while reducing side effects. These compounds, characterized by a unique closed ring at the fifth carbon position,[8] have shown promise as anti-convulsants, hypnotics, anesthetics, and anti-cancer agents (Fig. 1).[9,10]

Traditional synthetic approaches for spiro-barbiturates typically rely on ring-closure reaction methodologies which often require hazardous organic solvents and harsh reaction conditions, raising serious environmental and health concerns.[11–13] For example, Zheng and co-workers documented a phosphine-catalyzed method involving [3 + 2] and [4 + 2] annulation of ynones with barbiturate-derived alkenes, providing access to structurally diverse and potentially bioactive spirobarbiturates.[14] Although the reaction led to the formation of desired products with moderate to good yield, the use of toluene as the solvent and the requirement of high temperature and an inert atmosphere raised concerns regarding the green and sustainable applicability of this method. Similarly, Chen and co-workers employed a domino [3 + 2] aza-MIRC (Michael Induced Ring Closure) reaction between barbiturate-derived alkenes and *N*-alkoxy α-haloamides to synthesize a diverse array of spirobarbiturate-pyrrolidinones which were obtained in excellent yields (>99%).[15] The use of K_2CO_3 as a base and DCM as the solvent under ambient conditions enabled efficient cycloaddition without the need for strong bases or fluorinated solvents, likely due to the high intrinsic acidity of the *N*-alkoxy α-haloamides. Despite its efficiency, the use of DCM, a halogenated solvent, posed serious limitations with regard to its large-scale application owing to environmental and regulatory concerns. More recently, Khurana *et al.* employed THF as a solvent for a one-pot, three-component reaction involving triphenylphosphine, dialkyl acetylenedicarboxylates, and 5-arylidene-1,3-dimethylpyrimidine-2,4,6-triones to synthesize triphenylphosphanylidene-7,9-diazaspiro[4.5]dec-1-ene-2-carboxylates.[16] Furthermore, a comprehensive review by Magoo *et al.* presents a comparative study of various synthetic protocols of spirobarbiturates having 5-membered rings with their distinctive features.[17] Apart from the issues of use of toxic reagents, many of the reported methodologies also suffer from prolonged reaction times, low yields and poor selectivity. Our report addresses this issue by employing green chemistry principles to synthesize spiro-barbiturates by the reaction of triphenyl phosphine with dimethyl acetylene dicarboxylate and arylidene barbiturates using cyclopentyl methyl ether (CPME) as the solvent under room temperature conditions. CPME is favored as a green solvent due to its low toxicity, high boiling point, low peroxide-forming tendency, and recyclability, aligning with green solvent selection frameworks such as GSK and CHEM21.[18] Its use mitigates hazards associated with conventional ethers like THF and environmentally persistent halogenated solvents. This approach not only reduces environmental impact but also offers better yields and recyclability which can also be gauged from the green chemistry metrics presented herein. Furthermore, the docking and simulation analyses provide insights into the binding affinities and interactions of spiro-barbiturates, emphasizing their potential as neuronal drugs for anxiety and depression.

Results and discussion

Research design

This study presents an efficient one-pot, three-component synthesis of triphenylphosphanylidene-7,9-diazaspiro[4.5]dec-1-ene-2-carboxylate derivatives (**IVa–d**). To optimize the reaction conditions, 5-(4-fluorobenzylidene)-1,3-dimethylpyrimidine-2,4,6(1*H*,3*H*,5*H*)-trione (**Ia**) was chosen as the model substrate which was synthesized beforehand *via* the condensation reaction between 4-fluorobenzaldehyde and 1,3-dimethylbarbituric acid according to the reported procedure (Scheme 1).[19]

To synthesize the spiro-barbiturate compounds (**IV**), arylidene-1,3-dimethylpyrimidine-2,4,6(1*H*,3*H*,5*H*)-triones (**I**) were reacted with dimethylacetylenedicarboxylate (**II**) and triphenylphosphine (**III**), probing a variety of green solvents – anhydrous glycerol, PEG-400, water and cyclopentyl methyl ether (CPME). The reaction was also tried under neat conditions (Table 1). CPME gave the best results in terms of the reaction times and the ease of reaction work-up for the extraction of desired products; thus, it was considered the green solvent of choice for the synthetic methodology (Scheme 2). In our initial screening, we explored polar, protic (hydroxylic) solvents such

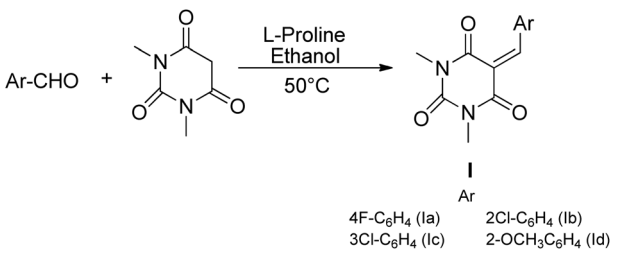

Scheme 1 Synthesis of benzylidene-1,3-dimethylpyrimidine-2,4,6(1*H*,3*H*,5*H*)-triones.

Table 1 Optimization of reaction conditions for the synthesis of methyl 1-(4-fluorophenyl)-7,9-dimethyl-4,6,8,10-tetraoxo-3-(triphenylphosphoranylidene)-7,9-diazospiro[4,5]dec-1-ene-2-carboxylate[a]

S. no.	Solvent	Time (h)	Yield (%)
1	Anhydrous glycerol	24	45
2	PEG-400	24	52
3	Water	24	21
4	No solvent[b]	24	—[c]
5	Cyclopentyl methyl ether (CPME)	4	89

[a] Reaction was carried out using 5-(4-fluorobenzylidene)-1,3-dimethylpyrimidine-2,4,6(1*H*,3*H*,5*H*)-trione (1.0 mmol), dimethyl acetylene dicarboxylate (1.2 mmol) and triphenylphosphine (1.1 mmol) at RT. [b] Neat conditions. [c] Incomplete reaction with a number of spots in TLC.

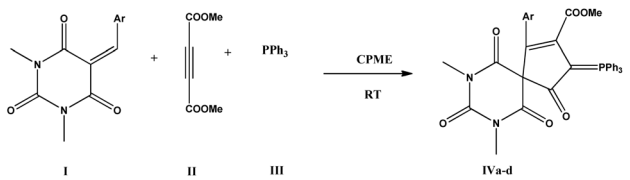

Scheme 2 Synthesis of spiro-barbiturate compounds (IV).

as ethanol and water based on their established green characteristics including low toxicity, biodegradability, and renewability as part of our effort to identify safer alternatives to conventional solvents like THF and toluene, which are non-polar, aprotic, volatile, and toxic.

Significant yield of the desired product methyl 1-(4-fluorophenyl)-7,9-dimethyl-4,6,8,10-tetraoxo-3-(triphenylphosphoranylidene)-7,9-diazaspiro[4.5]dec-1-ene-2-carboxylate **IVa** was obtained when the reaction was carried out in CPME at room temperature for 4 hours. The conditions were extended to synthesize spirobarbiturate compounds **IVb–d** which were obtained in good to excellent yields (Table 2). The products thus obtained were fully characterized using IR and ^{1}H NMR spectra.

Green chemistry considerations

It is well known that the processes that cannot be measured cannot be controlled.[20] Control in green chemistry should be understood as a possibility to select the greenest option. The significance of green chemistry metrics lies in their ability to quantify and evaluate how "green" a chemical process is, providing a scientific and standardized way to assess environmental and economic performance. These metrics are essential tools in making chemical research and manufacturing more sustainable by predicting how a certain change in a synthesis path, such as elimination or replacement of a solvent, would influence its environmental impact.[21]

Table 2 Exploration of substrate scope for the synthesized derivatives

S. no.	R	Ar	Product	Time (h)	Yield (%)
1	Me	4-FC_6H_4	**IVa**	4	89
2	Me	2-ClC_6H_4	**IVb**	4	87
3	Me	3-ClC_6H_4	**IVc**	3.5	88
4	Me	2-$OCH_3C_6H_4$	**IVD**	4.5	86

Table 3 Green metrics applied to the current synthetic protocol for obtaining spiro-barbiturates

Product	AE (%)	CE (%)	Y_E	MI	RME	EF
IVa	95.19	88.45	78.31	3.27	0.49	3.27
IVb	95.30	82.43	79.83	3.29	0.48	3.29
IVc	95.30	77.41	78.12	3.37	0.46	3.37
IVd	95.27	75.51	75.88	3.43	0.46	3.43

For the evaluation of the environmental impact of this synthesis, some of the important and relevant green chemistry metrics that have been utilized are shown below and the results are summarized in Table 3.

Atom economy (AE). AE is a very important metric for assessing the efficiency and greenness of a chemical reaction as it quantifies the atoms of the reactants that end up in the product and by-products.[22]

$$\mathrm{AE} = \frac{\text{molar mass of product}}{\text{total molar mass of all reactants}} \times 100\%$$

Carbon efficiency (CE). CE is defined as the percentage of carbon from the reactants that is retained in the final product. It serves as a valuable metric for evaluating the environmental impact of a chemical process. This parameter is especially important in the pharmaceutical industry, where constructing carbon skeletons is central to molecular design.

$$\mathrm{CE} = \frac{\text{amount of carbon in product}}{\text{total carbon in reactants}} \times 100\%$$

Effective mass yield (Y_E). Y_E is defined as the percentage of the mass of the desired product relative to the total mass of all non-benign (*i.e.*, non-toxic or hazardous) materials used in its synthesis. This metric integrates both efficiency and safety into the assessment by emphasizing the proportion of the final product derived from materials that pose environmental or health concerns.

$$Y_E = \frac{\text{mass of products}}{\text{mass of non-benign reagents}} \times 100\%$$

Mass intensity (MI). MI quantitatively incorporates the effects of yield, stoichiometric efficiency, and the masses of solvents and reagents employed in a reaction by focusing on the total mass of materials used to produce a given mass of the product. For an ideal synthesis, MI has a value of 1.

$$\mathrm{MI} = \frac{\text{total mass used in the process (excluding water)}}{\text{mass of the product}} \times 100\%$$

Reaction mass efficiency (RME). RME is a more comprehensive measure than atom economy as it takes into account both atom economy and reaction yield, measuring the ratio of the mass of the desired product to the mass of all the reactants utilized in a reaction.

$$\mathrm{RME} = \text{atom economy} \times \text{yield} \times \frac{1}{\mathrm{SF}}$$

where $\mathrm{SF} = \text{stoichiometric coefficient} = 1 + \frac{\text{atom economy} \times \text{total mass of excess reagents}}{\text{theoretical mass of the product}} \times 100\%$

***E*-Factor (EF).** Proposed by Roger Sheldon, this parameter quantifies the waste generated for a given mass of product and is used by many industries for assessing waste.

$$E\text{-Factor (EF)} = \frac{\text{mass of waste}}{\text{mass of desired product}}$$

As evident from calculations presented in Table 3, the devised protocol shows high atom economy and carbon efficiency in all cases. The methodology exploits one of the most important principles of green chemistry *i.e.* the use of safer solvents and auxiliaries by employing CPME as the solvent of choice, instead of toxic solvents such as THF and toluene that are generally used for synthesis of such compounds. Furthermore, CPME was recovered after the reaction by rotary evaporation and could be reused without significant loss of yield, making the process all the more sustainable. A comparative analysis done with the previously reported protocol employing THF as the solvent[16] shows that both the protocols offer significant advantages of high atom economy, carbon efficiency and reaction mass efficiency, but the present protocol offers a distinctive environmental advantage due to the choice of solvent. Despite its derivation from non-renewable feedstocks, CPME is recognized for its low toxicity, reduced peroxide formation tendency, high boiling point, and low environmental persistence (Table S1). It stands out as a more sustainable alternative to commonly used ethereal solvents such as diethyl ether (Et_2O), THF, 1,2-dimethoxyethane (DME), dioxane, and methyl *tert*-butyl ether (MTBE). It is imperative to mention here that CPME has been ranked on the GSK and CHEM21 lists of preferred solvents based on low toxicity, good stability, and low risk for peroxide formation; hence it is more sustainable compared to the traditional commonly used ethers.[23]

Also, performing the synthesis of spirobarbiturates at room temperature follows the sixth principle of green chemistry *i.e.* designing an energy efficient process. Even the synthesis of the precursor (Ia-d) utilizes a greener catalyst L-proline instead of DBU or NaOH for the synthesis of alkenes from dimethyl barbituric acid and aromatic aldehydes. It also takes into account that the least amount of waste is generated as a side product as water is the major side product in alkene synthesis. The simplicity of operation, mild reaction conditions, and high yields obtained without chromatographic purification render this method suitable for both laboratory-scale and industrial synthesis.

Molecular docking

Molecular docking of the spirobarbiturate compounds **IVa–d** with the neurotransmitter receptors, glutamate receptor (1yae), Ca^{2+} channel complex (3jbr), Ca^{2+} channel β-2 subunit (4dex), proton dependent potassium channel (4lcu), glutamate 2/3 receptor heterotetramer (5ide), Na^{+} channel β-1 subunit (5xsy), GluN1/GluN2A NMDA receptor (7eoq) and GABAA (gamma-aminobutyric acid) α1β3γ2 receptor (7qne), was performed to predict their binding affinity and detailed interactions. The docking was performed using InstaDock, a single click molecular docking tool that automizes the entire process of molecular docking-based virtual screening.[24] The binding affinities between the ligand and protein were calculated using the QuickVina-W[25] and Modified AutoDock Vina[26] programs which use a hybrid scoring function (empirical + knowledge-based) in docking calculations and a blind search space for the ligand. The pK_i, the negative decimal logarithm of the inhibition constant,[27] was calculated from the ΔG parameter while using the following formula:

$$\Delta G = RT(\ln K_{\mathrm{ipred}})$$

$$K_{\mathrm{ipred}} = e(\Delta G/RT)$$

$$pK_i = -\log(K_{\mathrm{ipred}})$$

where ΔG is the binding affinity (kcal mol^{-1}), R (gas constant) is 1.98 cal $(mol\ K)^{-1}$, T (room temperature) is 298.15 K, and K_{ipred} is the predicted inhibitory constant. Ligand efficiency (LE) is a commonly applied parameter for selecting favorable ligands by comparing the values of average binding energy per atom.[28] The following formula was applied to calculate LE:

$$\mathrm{LE} = -\Delta G/N;$$

where LE is the ligand efficiency (kcal per mol per non-H atom), ΔG is binding affinity (kcal mol^{-1}) and N is the number of non-hydrogen atoms in the ligand. The obtained docked poses of each spirobarbiturate on GABA(A)R were re-validated by using DiffDock which uses a non-Euclidean diffusion generative model, with a top 1 success rate of 38% on PDB-Bind which is more efficient than the conventional docking (23%) and deep learning algorithms (20%). The top ranked model pose for each spirobarbiturate on GABA(A)R was used for molecular dynamics simulations.[29] Table 4 shows a summary of receptor–ligand interactions and binding energies for all spirobarbiturates (**IVa–d**) with a series of neurotransmitter-related targets. The trend from the data indicates that **IVd**, which has a methoxy group at the *ortho*-position of the aryl ring, has consistently the strongest binding interactions with a variety of receptors, most notably the GABA(A) receptor (−8.6 kcal mol^{-1}, 3 H-bonds) and the NMDA receptor (−8.9 kcal mol^{-1}, 1 H-bond). This implies that the electron-donating methoxy group can potentially increase electron density at crucial sites for hydrogen bonding and pi–pi stacking, enhancing overall binding affinity and interaction specificity. Likewise, **IVa** with a *para*-fluoro substituent exhibits respectable binding at the majority of receptors, particularly

Table 4 Receptor ligand interactions for spirobarbiturates IVa–d

S. no.	Receptor	Ligand	Binding energy (kcal mol^{-1})	Type of interaction	Amino acids involved	Docking interaction analysis figure
1	7qne ($GABA_A$ α1β3γ2 receptor)	**IVa**	−8.1	1 H bond	L297	Fig. 2(a)
		IVb	−8.2	4 H bonds	R180, K156, and A45	
		IVc	−7.8	No bond		
		IVd	−8.6	3 H bonds	E168, R180, and S46	
2	7eoq	**IVa**	−10.1	5 H bonds	R694, E707, and R489	Fig. 2(b)
	(GluN1/GluN2A NMDA receptor)	**IVb**	−9.8	No bond		
		IVc	−9.4	2 H bonds	E522 and R431	
		IVd	−8.9	1 H bond	E734	
3	1yae (glutamate receptor)	**IVa**	−7.7	1 H bond	T520	Fig. 2(c)
		IVb	−8.2	3 H bonds	Y521, T520, and F693	
		IVc	−8.2	1 H bond	T520	
		IVd	−7.8	2 H bonds	A518 and T520	
4	5ide (glutamate 2/3 receptor	**IVa**	−7.2	1 H bond	F663	Fig. 2(d)
	heterotetramer)	**IVb**	−7.3	2 H bonds	I615 and N791	
		IVc	−7.9	2 H bonds	I227 and F224	
		IVd	−7.3	2 H bonds	V252 and F255	
5	3jbr (Ca^{2+} channel complex)	**IVa**	−7.9	No bonds		Fig. 2(e)
		IVb	−8.7	3 H bonds	E100 and L118	
		IVc	−8.2	No bonds		
		IVd	−8.8	1 H bond	F146	
6	4dex (Ca^{2+} channel β-2 subunit)	**IVa**	−7.2	5 H bonds	R228, D384, and A336	Fig. 2(f)
		IVb	−7.5	5 H bonds	R228, D384, and K91	
		IVc	−7.5	5 H bonds	R228, D384, and P337	
		IVd	−7.4	1 H bond	Y402	
7	4lcu	**IVa**	−8.5	2 H bonds	F29 and T30	Fig. 2(g)
	(proton dependent potassium channel)	**IVb**	−7.2	1 H bond	S88	
		IVc	−7.3	1 H bond	G8	
		IVd	−7.8	1 H bond	E153	
8	5xsy (Na^+ channel β-1 subunit)	**IVa**	−8.6	No bond		
		IVb	−8.7	No bond		
		IVc	−8.7	No bond		
		IVd	−8.2	No bond		

NMDA (−10.1 kcal mol^{-1}, 5 H-bonds), suggesting that electronegative fluorine might position the molecule favorably within the binding pocket and contribute to polar interactions.

The activities of **IVb** and **IVc**, both bearing chloro substituents in *ortho* and *meta* positions respectively, are more disparate. **IVb** exhibits strong hydrogen bonding with glutamate and GABA(A) receptors, probably because of favorable steric placement of the *ortho*-chloro group, whereas **IVc**, bearing a *meta*-chloro group, acts worst in hydrogen bonding and overall interaction with the GABA(A) receptor.

Considered in combination, the information indicates that substituent electronics and positions are key determinants of receptor affinity and quality of interaction. *Ortho*-methoxy and *para*-fluoro substituents seem to maximize ligand orientation and interaction with receptor binding sites, perhaps through increased hydrogen bonding and polar interactions, rendering **IVd** and **IVa** the best candidates for continued development as CNS-active drugs.

Fig. 2(a)–(g) illustrate the best-docked conformations and key interactions of fluoro, chloro (*ortho*/*meta*), and methoxy-substituted spirobarbiturates with GABA(A), NMDA, glutamate, and ion channel receptors, highlighting variations in hydrogen bonding and binding affinities. For the sodium channel β-1 subunit (PDB ID: 5xsy), none of the spirobarbiturate derivatives (**IVa–IVd**) exhibited any specific hydrogen bonding or polar interactions within the binding pocket. As a result, no interaction diagrams were generated for this receptor.

Molecular dynamics simulations (MDS) and MMGBSA calculations

The MDS of spirobarbiturates **IVa–d** with the GABA A receptor was performed for 100 ns each using the LiGRO tool along with GROMACS 5.1.5. The docked complexes were solvated in a TIP3P water-filled cubical box with an edge distance of 1 nm and 0.15 M NaCl to neutralize the system. The systems were energy minimized using 1500 steps of the steepest descent algorithm. The AMBER99SB and GAFF2 (with the BCC charge model) force fields were used for proteins and ligands respectively. The systems were ensured to be well equilibrated for 2 ns each in the NVT (310.15 K) and NPT (1 atm) ensembles followed by an MDS production run of 100 ns. The trajectory analysis was done using standard GROMACS tools and PyMOL v.2.5. The end-state binding free energy calculations (MMGBSA) were done using the gmx_MMPBSA tool on the 1000 frames extracted from the MDS

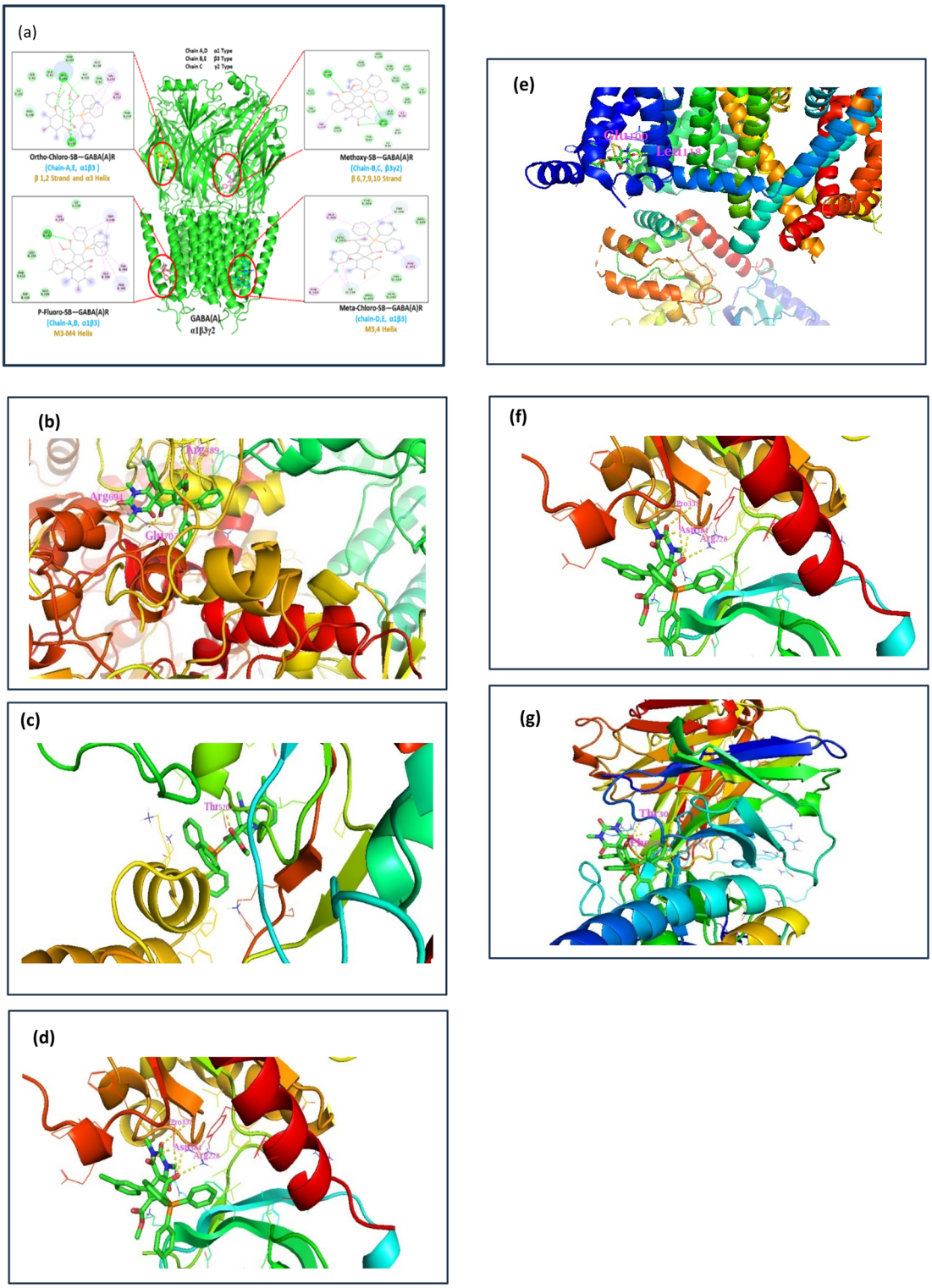

Fig. 2 (a)–(g) Schematic 2D representations of receptor–ligand interactions between spirobarbiturates and the GABA(A) receptor and its allied neurotransmitter receptors.

trajectories. For enthalpic contributions, the iGB model 2 with an internal dielectric constant value of 2 was used and the interaction entropy was calculated on the last 25% of the frames.

The molecular dynamics simulation of spirobarbiturates (SBs) with GABA(A)R was run to find their mode of action and probable binding sites on GABA(A)R. Our results were in tune with the results obtained by Ghit *et al.*, 2021, where they found that barbiturate compounds bind to the αβ and βγ chains. Similarly, we found that our designed SBs follow a similar trend and bind to the α1β3 (**IVa–c**) and β3γ2 (**IVd**) subunits. As

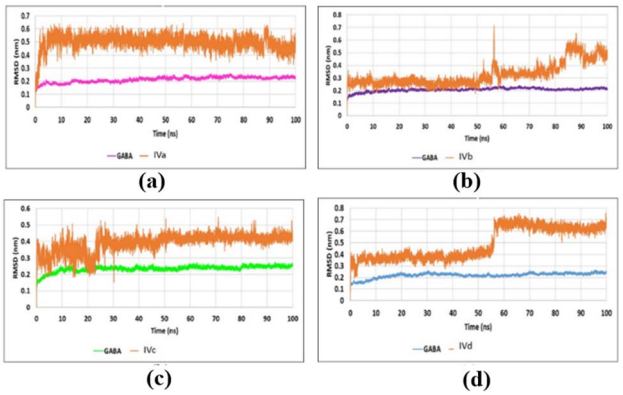

Fig. 3 (a)–(d) RMSD plots of GABA(A) receptor–spirobarbiturate complexes over 100 ns of simulation showing the structural stability of the receptor and ligands. Each plot corresponds to one of the four spirobarbiturates (**IVa**, **IVb**, **IVc**, and **IVd**) indicating ligand convergence and receptor–ligand complex stabilization.

observed from the RMSD plots, GABA(A)R maintained a stable structure in complex with SBs with RMSD less than 2.5 Å in each case. SBs showed RMSD ranging from 3–7 Å to achieve the stable conformation by the end of the simulation with **IVa** and **IVc** showing less fluctuations as compared to **IVb** and **IVd** (Fig. 3(a)–(d)).

From the R_g plot, a slight expansion in the GABA(A)R was observed initially in complex with **IVc** and **IVd** while a slight expansion in GABA(A)R was observed in complex with **IVb**, whereas GABA(A)R maintained stable R_g in complex with **IVa** (Fig. 4(a) and (b)).

The major stabilizing interactions of SBs with GABA(A)R were hydrophobic in nature and formed the least number of hydrogen bonds. From the MMGBSA binding energy scores, **IVd** (-53.20 ± 5.81 kcal mol^{-1}) showed the highest binding affinity with GABA(A)R followed by **IVc** (-49.97 ± 3.74 kcal mol^{-1}), **IVa** (-46.53 ± 3.34 kcal mol^{-1}) and **IVb** (-31.42 ± 7.86 kcal mol^{-1}).

A comparative overview of docking scores (ΔG) and MMGBSA binding free energies (ΔG_MMGBSA) for the spirobarbiturate series (**IVa–IVd**) provides valuable insights into their dynamic receptor interactions and stability profiles (Table 4).

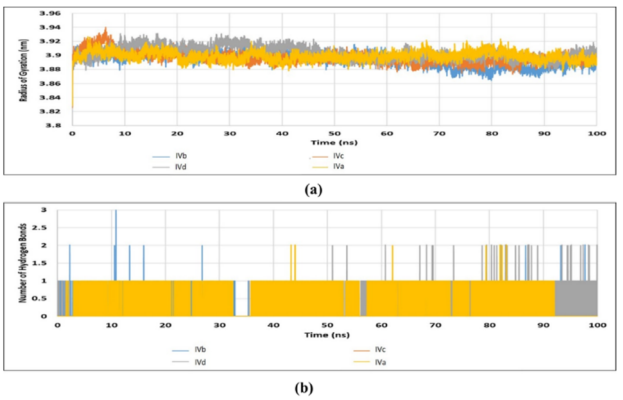

Fig. 4 (a) and (b) Radius of gyration (R_g) plots of the GABA(A) receptor in complex with each spirobarbiturate.

IVd showed a high docking score against GABA(A) (-8.6 kcal mol^{-1}) and NMDA (-8.9 kcal mol^{-1}), where it established several hydrogen bonds with residues like E168 and R180. These static interactions were further confirmed by MDS and MMGBSA analysis, where **IVd** had the best free energy of binding (-53.20 ± 5.81 kcal mol^{-1}), which reflects continuous interaction and conformational stability in the receptor binding pocket over time.

IVa also showed consistent performance with good docking scores (-8.1 kcal mol^{-1} for GABA(A), -10.1 kcal mol^{-1} for NMDA) and good MMGBSA energy (-46.53 ± 3.34 kcal mol^{-1}), indicating stable complex formation throughout simulations. Its fluorine atom probably facilitates polar interactions while having an optimal steric profile.

Conversely, **IVb** had very good docking scores (-8.2 to -9.8 kcal mol^{-1}), but its MMGBSA energy was much lower (-31.42 ± 7.86 kcal mol^{-1}). This indicates that although it makes good initial contacts, **IVb** might experience suboptimal orientation or destabilization in the long term, perhaps because of steric hindrance or solvent effects within the binding site.

Intriguingly, **IVc**, with more feeble docking interaction with GABA(A) (-7.8 kcal mol^{-1}, no H-bonds), was ranked second in MMGBSA energy (-49.97 ± 3.74 kcal mol^{-1}). This suggests that its binding mode would be enhanced at equilibration to result in good enthalpic and entropic contributions not accessible to static docking.

These results affirm the need for combining molecular dynamics simulations with docking research to learn about ligand–receptor behavior in depth. Docking gives good starting predictions, and MDS and MMGBSA show the dynamic stability and actual binding of each compound to prioritize promising candidates for conducting *in vitro* screening. Table 5 emphasizes data from both MD simulation and molecular docking.

Spectral analysis

The IR spectrum of the synthesized compounds showed a characteristic band between 1691 and 1708 cm^{-1} confirming the presence of C=O groups. The FTIR spectrum of representative compound **IVa** (Fig. S1) indicates a peak near 1652 cm^{-1} corresponding to amide C=O stretching frequency. The peak at 1206 cm^{-1} corresponds to C–O stretching frequency. The peak at 1043 cm^{-1} corresponds to C–F stretching frequency, indicating the fluoro group's presence. A further peak at 1531 cm^{-1} corresponds to aromatic C=C stretching frequency. Peaks between 600 and 900 cm^{-1} correspond to aromatic C–H bending. FTIR spectra of **IVb–d** are also provided in the SI (Fig. S3, S5 and S7).

For the characterization of the synthesized spirobarbiturates, ^{1}H-NMR was used to identify the distinct protons in the compound. By analyzing chemical shifts, coupling patterns, and integration values, the structure of the synthesized compounds could be confirmed. The ^{1}H NMR spectrum showed three methyl protons of the ester group appearing as a singlet at δ 2.82. The methyl protons of 1,3-dimethyl barbituric acid also appeared as a singlet at δ 3.24 (Fig. S2). The 19 aromatic protons appeared in the range δ 7.77–6.87 as shown in

Table 5 Docking *vs.* MD/MMGBSA insights

Compound	Docking energy (GABA(A))	MMGBSA energy	H-Bonds (GABA(A))	RMSD stability
IVa	−8.1 kcal mol^{-1}	−46.53 kcal mol^{-1}	1	Low
IVb	−8.2 kcal mol^{-1}	−31.42 kcal mol^{-1}	4	Moderate
IVc	−7.8 kcal mol^{-1}	−49.97 kcal mol^{-1}	0	Low
IVd	−8.6 kcal mol^{-1}	−53.20 kcal mol^{-1}	3	Moderate

the SI. The 1H NMR spectrum of **IVb–d** is also provided in the SI (Fig. S4, S6 and S8).

Integrated computational insights: docking, dynamics, and energy landscapes

What stands out in this study is how each computational layer is built on the last—offering both validation and deeper context. We began with docking to get a sense of static binding affinity. **IVd** emerged early as a strong candidate, with ΔG values consistently better than those of its analogues across several neurotransmitter receptors, particularly GABA(A) and NMDA. Once we ran molecular dynamics (100 ns, GROMACS *via* LiGRO), a more textured picture emerged. Ligand RMSDs suggested differential stability across analogues—**IVa** and **IVc** were comparatively steady, whereas **IVb** and **IVd** showed more movement before stabilizing. Interestingly, this fluctuation didn't always correlate with docking scores, a reminder that high initial binding doesn't guarantee long-term compatibility within the dynamic binding pocket.

The MMGBSA results sharpened the distinctions. **IVd** had the lowest binding free energy (−53.20 ± 5.81 kcal mol^{-1}), followed by **IVc**, **IVa**, and then **IVb**. But **IVc**'s strong MMGBSA score was obtained despite a weaker docking profile. This divergence caught our attention. This suggests that **IVc** may adopt a more favorable orientation over time, not captured in docking but revealed through dynamics—a small but useful caution against over-reliance on docking metrics alone.

Mapping residue-level interactions gave us further clarity. Key contacts—Arg180, Glu168, and Ser46—kept showing up, especially for **IVd**. These residues align well with known GABAergic pharmacophores (see Ghit *et al.*, 2021), which gives us some confidence that our ligand–receptor hypotheses are grounded in structural precedent. The substituent-dependent trends, especially the superior performance of *ortho*-methoxy and *para*-fluoro groups, suggest specific design rules for SAR optimization. We didn't test those experimentally (yet), but the trend is consistent enough to consider pursuing. One could easily imagine designing a follow-up series around these motifs. All told, this multi-pronged computational workflow not only confirms **IVd** as a lead candidate but also reveals nuances that a single method might miss. It also affirms the value of combining green synthetic chemistry with *in silico* screening—especially when teaching or training students in modern drug discovery workflows. There's educational value in seeing how assumptions evolve when you move from static to dynamic models, and that's something no table of docking scores can really teach on its own.

Comparison with literature precedents

As highlighted in the Introduction section, while most of the methods involve a similar ring closure approach, yet many of them involve toxic reagents/solvents *etc.* While CPME which is reported in the present protocol is not entirely non-toxic, it presents notable green advantages over THF and toluene, including:

- Lower peroxide-forming potential, which enhances laboratory safety and chemical stability;
- Higher hydrophobicity and stability under acidic and basic conditions, making it a more robust and reusable solvent;
- Better compliance with green solvent selection guides, such as those recommended by pharmaceutical industries.

Experimental

Synthesis

A mixture of 5-arylidene-1,3-dimethylpyrimidine-2,4,6(1*H*,3*H*,5*H*)-trione (1.0 mmol) and dimethyl acetylene dicarboxylate (1.2 mmol) was stirred magnetically in CPME (3 ml) at room temperature. Triphenylphosphine (1.1 mmol), dissolved in 2 ml of CPME, was added portionwise for 10 min whilst stirring. The progress of the reaction was monitored over 1 hour time intervals using ethyl acetate : petroleum ether (30 : 70, v/v) as an eluent. After completion of the reaction, the solvent was evaporated and the solid product obtained was recrystallized and filtered using ethanol (∼2 ml). The reaction was completed in 3.5–4.5 h and significant yields of the desired products were obtained. All the products were fully characterized by IR and NMR spectroscopy and the data were compared with the previous report.[16]

Conclusion

In this study, an environmentally benign synthetic procedure for spiro-barbiturates was established, through a one-pot, three-component reaction under ambient conditions employing cyclopentyl methyl ether (CPME) as a green solvent. The given protocol meets some of the fundamental principles of green chemistry such as waste prevention, atom economy, safer solvents and auxiliaries, energy efficiency, and catalysis and hence reduces both environmental and operational risks. The reaction operates under room temperature conditions without the requirement for chromatographic purification and, as such, is inherently more energy-efficient and practical for scale-up.

The procedure showed superior atom economy, optimal carbon efficiency, and low *E*-factors that reflect reduced waste

generation and high material throughput. In comparison to conventional techniques using toxic, environmentally hazardous solvents such as THF, acetonitrile, or DMF—even under reflux conditions or at increased temperatures—this procedure offers cleaner, safer, and more economical access to medicinally important heterocycles.

In addition, CPME, the preferred solvent, concurs with various green solvent selection guidelines as a result of its low toxicity, high boiling point, low tendency towards peroxide formation, and reusability. Its application precludes the hazards inherent with traditional ethers like peroxide formation in THF or environmental persistence in halogenated solvents.

Overall, this research illustrates how sustainable and innovative synthetic methods can be combined with cheminformatics to provide biologically relevant scaffolds. This study lays the groundwork for subsequent *in vitro* and *in vivo* investigations to fully assess the therapeutic potential of the compounds. Methoxy-substituted spiro-barbiturate (**IVd**) proved to be an especially promising hit, with high binding affinity and stability towards GABA(A) receptors *in silico*. As a whole, this study provides a useful framework for the convergence of green chemistry and computational drug discovery research.

Conflicts of interest

There are no conflicts to declare.

Data availability

The data underlying this study are available in the Supporting Information (SI). See DOI: **https://doi.org/10.1039/d5su00343a**.

Acknowledgements

DM, AS, RJ, SD, SMG, SN and Kirti from Hindu College are thankful to the DBT Star College Scheme; SS, SG and KWM are thankful to the Department of Chemistry, Miranda House College, Department of Chemistry, University of Delhi and Department of Chemistry, Dyal Singh College, University of Delhi, respectively for administrative and moral support. DM and SMG are also grateful to Hindu College for the Innovation Project – IP 2019-20/SC-11 grant. SS is grateful to Miranda House for the grant under MHR & D Cell: R&D-17/2024.

Notes and references

1 P. Anastas and N. Eghbali, *Chem. Soc. Rev.*, 2010, **39**(1), 301–312.
2 I. T. Horvath and P. T. Anastas, *Chem. Rev.*, 2007, **107**, 2167.
3 P. T. Anastas and J. C. Warner, *Green Chemistry: Theory and Practice*, Oxford University Press, Oxford, 1998, vol. 160, ISBN 0-19-850234-6.
4 I. Ito, K. Sakimura, M. Mishina and H. Sugiyama, *Neurosci. Lett.*, 1996, **203**(1), 69–71.
5 A. L. Hopkins, G. M. Keserü, P. D. Leeson, D. C. Rees and C. H. Reynolds, *Nat. Rev. Drug Discovery*, 2014, **13**(2), 105–121.
6 E. E. Benarroch, *Neurology*, 2007, **68**(8), 612–614.
7 M. Jazvinscak Jembrek and J. Vlainic, *Curr. Pharm. Des.*, 2015, **21**(34), 4943–4959.
8 N. N. Pesyan, S. Noori, S. Poorhassan and E. Şahin, *Bull. Chem. Soc. Ethiop.*, 2014, **28**(3), 423–440.
9 E. M. Galati, M. T. Monforte, N. Miceli and E. Raneri, *Il Farmaco*, 2001, **56**(5–7), 459–461.
10 R. K. Bhaskarachar, V. G. Revanasiddappa, S. Hegde, J. P. Balakrishna and S. Y. Reddy, *Med. Chem. Res.*, 2015, **24**, 3516–3528.
11 S. Liu, P. Shao, Y. Li, D. Wang, D. Hou, C. Qu and X. Yan, *Tetrahedron*, 2021, **79**, 131859.
12 A. S. Girgis, H. Farag, N. S. Ismail and R. F. George, *Eur. J. Med. Chem.*, 2011, **46**(10), 4964–4969.
13 V. N. Ingle, P. K. Gaidhane, S. S. Dutta, P. P. Naha and S. M. Sengupta, *J. Carbohydr. Chem.*, 2006, **25**(8–9), 661–671.
14 X. Gao, Z. Li, W. Yang, Y. Liu, W. Chen, C. Zhan and H. Guo, *Org. Biomol. Chem.*, 2017, **15**(25), 5298–5307.
15 C. C. Wang, J. Zhou, Z. W. Ma, X. P. Chen and Y. J. Chen, *Org. Biomol. Chem.*, 2019, **17**(41), 9200–9208.
16 S. Gupta, K. Aggarwal and J. M. Khurana, *ChemistrySelect*, 2018, **3**(15), 4110–4113.
17 D. Magoo, A. Srivastava, S. Gupta, R. Jain, S. Mondal Ghorai, Y. Dawer and S. Rani, *Mini-Rev. Org. Chem.*, 2024, **21**(2), 246–270.
18 U. Azzena, M. Carraro, L. Pisano, S. Monticelli, R. Bartolotta and V. Pace, *ChemSusChem*, 2019, **12**(1), 40–70.
19 S. Kulchat, K. Meguellati and J.-M. Lehn, *Helv. Chim. Acta*, 2014, **97**, 1219–1236.
20 R. A. Sheldon, *ACS Sustainable Chem. Eng.*, 2018, **6**(1), 32–48.
21 J. Martínez, J. F. Cortés and R. Miranda, *Processes*, 2022, **10**(7), 1274.
22 R. A. Sheldon, Atom efficiency and catalysis in organic synthesis, *Pure Appl. Chem.*, 2000, **72**(7), 1233–1246.
23 R. K. Henderson, C. Jiménez-González, D. J. Constable, S. R. Alston, G. G. Inglis, G. Fisher and A. D. Curzons, *Green Chem.*, 2011, **13**(4), 854–862.
24 A. Carvalho, S. J. Teixeira, L. Olim, S. D. Campanella and T. Costa, *Journal of Education and Training*, 2021, **63**(2), 195–213.
25 T. Mohammad, Y. Mathur and M. I. Hassan, *Briefings Bioinf.*, 2021, **22**(4), bbaa279.
26 N. M. Hassan, A. A. Alhossary, Y. Mu and C. K. Kwoh, *Sci. Rep.*, 2017, **7**(1), 15451.
27 O. Trott and A. J. Olson, *J. Comput. Chem.*, 2010, **31**(2), 455–461.
28 S. Shityakov and C. Förster, *Adv. Appl. Bioinf. Chem.*, 2014, 23–36.
29 W. Sieghart, J. Ramerstorfer, I. Sarto-Jackson, Z. Varagic and M. Ernst, *Br. J. Pharmacol.*, 2012, **166**(2), 476–485.